Practical Realization of Perfect Electromagnetic Conductor (PEMC) Boundaries using Ferrites, Magnet-less Non-reciprocal Metamaterials (MNMs) and Graphene

C. Caloz [#1], A. Shahvarpour [#1], D. L Sounas [#1], T. Kodera [*2], B. Gurlek [#1], N. Chamanara [#1]

[#] *Poly-Grames Research Center, École Polytechnique de Montréal, Montréal, Québec, H3T 1J4, Canada*
[1] `christophe.caloz@polymtl.ca`
[2] `attieh.shahvarpour@polymtl.ca`
[3] `dimitrios.sounas@polymtl.ca`
[5] `burak.gurlek@polymtl.ca`
[6] `nima.chamanara@polymtl.ca`

[*] *Department of Electrical Engineering, Yamaguchi University, Ube, Yamaguchi, 7558611, Japan*
[4] `tk@yamaguchi-u.ac.jp`

Abstract—**The perfect electromagnetic conductor (PEMC) was recently theoretically introduced by Lindell and Sihvola as a fundamental hypothetical electromagnetic medium. This papers proposes three related but distinct implementations – a ferrite, a magnet-less non-reciprocal metamaterial (MNM) and a graphene implementation – of a practical PEMC boundary. These implementations are all based on the combination of Faraday rotation and reflection from a conductive ground, but exhibit distinct and complementary features.**

I. Introduction

In 2005, Lindell and Sihvola introduced the concept of a perfect electromagnetic conductor (PEMC) by observing that, although apparently unphysical, such a medium would represent the simplest and the only absolutely isotropic[1] medium from the viewpoint of four-dimensional forms [1]. A PEMC may be defined in terms of the boundary conditions [2]

$$\mathbf{n} \times (\mathbf{H} + M\mathbf{E}) = 0, \tag{1a}$$

$$\mathbf{n} \cdot (\mathbf{D} - M\mathbf{B}) = 0, \tag{1b}$$

where $\mathbf{n}$ is the unit vector normal to the surface of the medium and M is its admittance. Equations (1) show that a PEMC is a generalization of a perfect electric conductor (PEC) and perfect magnetic conductor (PMC), where these two particular cases correspond to $M = \infty$ and $M = 0$, respectively. For the conditions (1) to be satisfied, the fields scattered by the medium must experience rotation, and hence a PEMC is necessarily gyrotropic. Furthermore, this gyrotropy must be non-reciprocal, as shown in [1] and [2], and as will be seen in Sec. II.

---

[1] An absolutely isotropic medium is a medium which remains the same (namely the same isotropic medium) for all observers moving with constant velocity.

The first valid realization of a PEMC boundary was reported and experimentally demonstrated in [3]. This PEMC is based on a ferrite slab on a conducting plane. The present paper discusses and compares three related – but distinct – PEMC boundary realizations: the aforementioned ferrite PEMC, a recently suggested magnetless-non-reciprocal metamaterial (MNM) based PEMC [4] and a graphene based PEMC.

II. General Principle

The three PEMC boundary realizations are based on the same principle, involving Faraday rotation and reflection from a PEC plane and introduced in [3] for the ferrite case. This realization principle is depicted in Fig. 1 for a generic gyrotropic medium placed on top of the PEC plane, represented in Fig. 1(a), where the PEMC boundary is achieved at the surface of the overall structure, at $z = 0$. For simplicity, consider the case of plane wave normal incidence, where Eqs. (1) reduce to

$$\mathbf{H} + M\mathbf{E} = 0, \tag{2}$$

indicating that the PEMC condition then reduces to collinearity between the electric and magnetic fields. For further simplicity, ignore at this point the effects of phase shifts across the gyrotropic medium and of multiple reflections in it. As the incident plane wave penetrates into the gyrotropic medium, it experiences Faraday rotation, where the electric and magnetic fields are rotated by the same angle θ. On the PEC plane, the electric field is flipped (phase reversal) under reflection whereas the magnetic field is reflected without direction change, according to PEC boundary conditions. The two reflected fields propagate then back to the surface, while
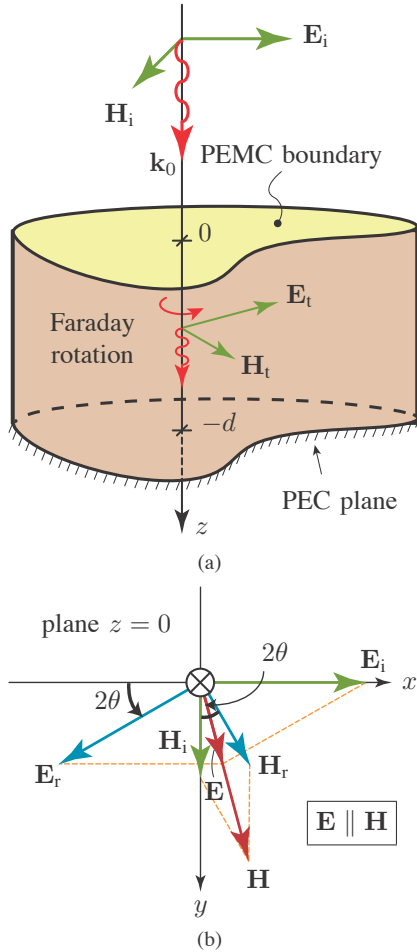
(a)

(b)

Fig. 1. Principle of PEMC boundary realization using Faraday rotation above a conductive plane. The particular case $\theta = \pi/2$ and $\theta = \pi/4$ corresponds to PMC and free-space ($M = 1/\eta_0$) PEMC conditions, respectively.
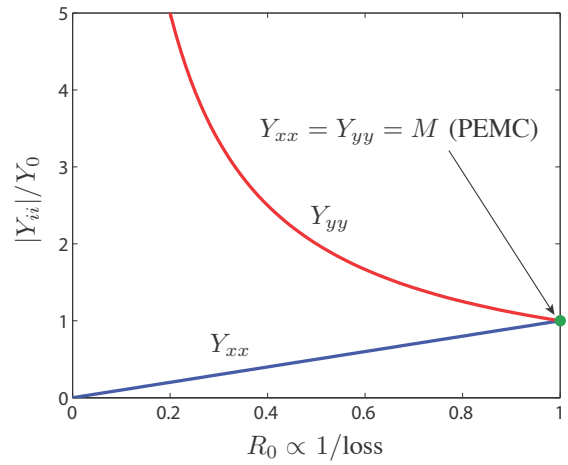

Fig. 2. Normalized two terms of $\bar{\bar{M}}$ in (3) versus R computed by (4) for $\theta = \pi/4$ (free-space PEMC). The normalized admittances in the directions parallel (x) and perpendicular (y) to the incident wave vary in the intervals $[0, 1]$ (0 for $\theta = 0$) and $[\infty, 1]$ (∞ for $\theta = 0$), respectively.

experiencing another θ rotation in the same direction with respect to z, as prescribed by the non-reciprocal nature of Faraday rotation. At the surface of the structure, the reflected fields, $\mathbf{E}_r$ and $\mathbf{H}_r$, add up to the incident fields, $\mathbf{E}_i$ and $\mathbf{H}_i$. This yields the vectorial field configuration shown in Fig. 1(b), where the total fields, $\mathbf{E} = \mathbf{E}_i + \mathbf{E}_r$ and $\mathbf{H} = \mathbf{H}_i + \mathbf{H}_r$, are seen to be collinear, and hence satisfying the PEMC condition (2).

Although the operation principle described in Fig. 1 explains the key concept of the proposed PEMC boundary, the effects of phase shifts, multiple reflections, loss, dispersion and possible oblique incidence alter the response of the structure, and must be taken into account by a complete electromagnetic analysis [3] for accurate design. In general, the condition (2) takes the dyadic (non-PEMC) form

$$\mathbf{H} + \bar{\bar{M}}\mathbf{E} = 0, \quad \text{with} \quad \bar{\bar{M}} = \begin{bmatrix} M_{xx} & M_{xy} \\ M_{yx} & M_{yy} \end{bmatrix}, \quad (3)$$

and the angle between $\mathbf{E}$ and $\mathbf{H}$, $\Delta\psi = \tan^{-1}(E_y/E_x) - \tan^{-1}(H_y/H_x)$, is non-zero. It becomes zero, and hence satisfies the PEMC condition (2), only when $E_y/E_x = H_y/H_x$ ($\Delta\psi = 0$), so that $\bar{\bar{M}}$ reduces to a scalar

M. Assuming the incident fields $(E_{ix}, E_{iy}) = (1, 0)$ and $(H_{ix}, H_{iy}) = (0, Y_0)$, the reflected fields at $z = 0$ are $(E_{rx}, E_{ry}) = (-R\cos 2\theta, R\sin 2\theta)$ and $(H_{rx}, H_{ry}) = (Y_0 R\sin 2\theta, Y_0 R\cos 2\theta)$, where R is the reflection coefficient at $z = 0$ and Y_0 is the admittance of the gyrotropic medium, assumed here to be matched to that of free space. The resulting total fields at $z = 0$ are $(E_x, E_y) = (1 - R\cos 2\theta, R\sin 2\theta)$ and $(H_x, H_y) = (Y_0 R\sin 2\theta, Y_0 + Y_0 R\cos 2\theta)$. We have then

$$Y_{xx} = -\frac{H_x}{E_x} = -Y_0 \frac{R\sin 2\theta}{1 - R\cos 2\theta}, \quad (4a)$$

$$Y_{yy} = -\frac{H_y}{E_y} = -Y_0 \frac{1 + R\cos 2\theta}{R\sin 2\theta}, \quad (4b)$$

where one must have $Y_{xx} = Y_{yy}$, in which case $M_{xx} = M_{yy} = M$ and $M_{xy} = M_{yx} = 0$, to satisfy the PEMC boundary condition[2]. It clearly appears in these relations that Y_{xx} and Y_{yy} differ from each other given a general reflection coefficient $R = R_0 e^{j\phi}$, including loss (R_0) and phase shift (ϕ). For instance, Figure 2 plots Y_{xx} and Y_{yy} versus R_0 for $\phi = 0$ (round-trip phase shift across the structure ignored or multiple of 2π); the PEMC boundary condition is achieved only in the absence of loss ($R_0 < 1$), since otherwise the reflected fields are reduced in magnitude and do not add up with the incident fields in a fashion to produce collinearity, as might be easily verified using the vector construction of Fig. 1(b).

III. FERRITE PEMC

In the case of the ferrite PEMC, the volume between the surface and the PEC plane is filled with a ferrite material, biased by a static magnetic field $\mathbf{H}_0 = H_0\hat{z}$ and hence

[2]In general, $Y_{ii} \neq M_{ii}$ ($i = x, y$), since $M_{ii} = -H_i/E_i|_{E_j=0, j\neq i}$, whereas $Y_{ii} = -H_i/E_i$ without any restriction on $E_j = 0, j \neq i$, and it is clearly apparent in the vectorial representation of Fig. 1(b) that $E_j \neq 0, j \neq i$.
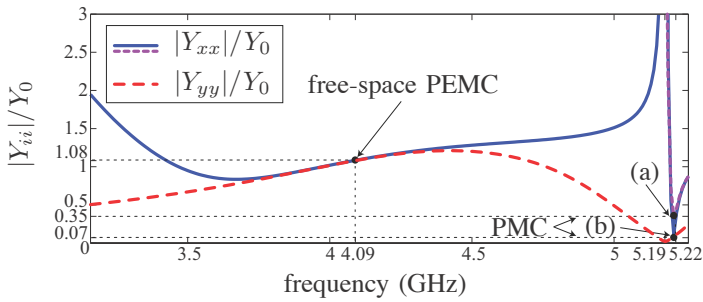
Fig. 3. Ferrite PEMC admittances versus frequency (exact electromagnetic result) for the following parameters: $d = 3$ mm, $\epsilon_r = 15$, $\mu_0 M_s = 0.188$ T, $\mu_0 H_0 = 0.2$ T, and for the line widths $\Delta H = 10$ Oe (a) and $\Delta H = 0$ Oe (b). The curves for (a) and (b) are undistinguishable from each other except for Y_{xx} near the PMC frequency (short-shaded curve). The phases (not shown) at the free-space PEMC and PMC frequencies are of $0°$ and $-18.9°$, respectively.

exhibiting the anisotropic response (Polder tensor)

$$\bar{\bar{\mu}} = \mu_0 \begin{pmatrix} \mu & j\kappa & 0 \\ -j\kappa & \mu & 0 \\ 1 & 0 & 0 \end{pmatrix}, \quad (5)$$

with $\mu = \mu_0[1 + \omega_0\omega_m/(\omega_0^2 - \omega^2)]$ and $\kappa = \mu_0\omega\omega_m/(\omega_0^2 - \omega^2)$, where $\omega_0 = \mu_0\gamma \mathbf{H}_0$ is the ferromagnetic resonance and $\omega_m = \mu_0\gamma M_s$, where γ is the gyromagnetic ratio (1.76×10^{11} rad/(Ts) for a ferrite) and M_s is the saturation magnetization [5]. In this case, Faraday rotation is continuous across the region $-d < z < 0$. The corresponding angle over a distance Δz is given by $\theta(\omega, \Delta z) = -[\beta_+(\omega) - \beta_-(\omega)]\Delta z/2$, with the right-handed and left-handed circularly polarized wavenumbers $\beta_\pm(\omega) = \omega\sqrt{\epsilon\mu_0[\mu(\omega) \pm \kappa(\omega)]}$.

Figure 3 plots the normalized admittances for the parameters indicated in the caption. It appears that quasi-perfect PEMC boundary are achieved at two points, a free-space PEMC at 4.09 GHz and a PMC PEMC at 5.22 GHz. The latter occurs closer to the resonance ($f_0 = 5.6$ GHz) and therefore exhibits a narrower bandwidth (visible) and a higher sensitivity to loss ($\Delta H = 10$ Oe here). The conductor-backed ferrite slab PEMC boundary was applied to the design of a transverse electromagnetic waveguide, with a cross-sectional size independent of the operation frequency in [3]. Note that the ferrite material could be potentially replaced by a ferromagnetic nanowire metamaterial [6] to suppress the need for a biasing magnet.

IV. MNM PEMC

The magnet-less non-reciprocal metamaterial (MNM) PEMC is the reflective MNM structure shown in Fig. 4. An MNM exhibits the same properties as a ferrite, its transistor-loaded ring particles supporting rotating radial magnetic dipole moments which emulate the rotating magnetic moments associated with electron spin precession in ferrites [7], [8]. As a result, the MNM PEMC operates essentially in the same way as the ferrite PEMC [4], except that its gyroropic activity is confined to the plane of the ring particles. Compared to the ferrite PEMC, the MNM PEMC provides the advantage of not requiring a biasing magnet and of being therefore compatible
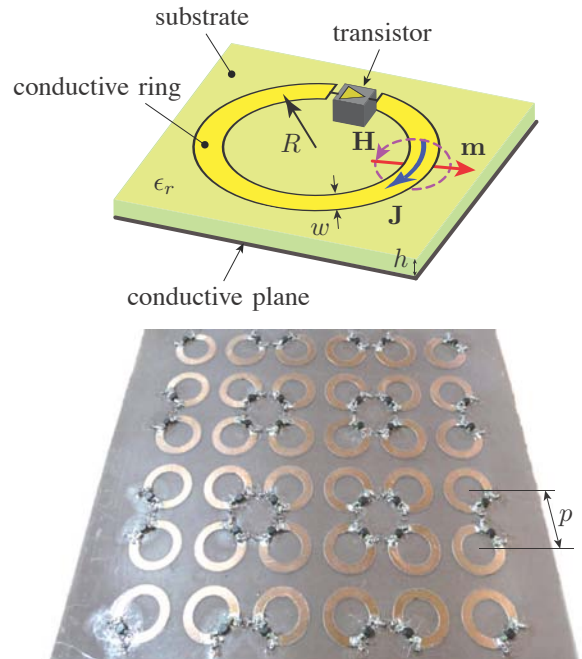

Fig. 4. Magnet-less non-reciprocal metamaterial (MNM) PEMC. Unit cell (top) and experimental prototype (bottom).

with MIC and MMIC technologies. A non-reciprocal leaky-wave antenna using such a material was reported in [9] and several other applications have been recently suggested. The MNM is characterized by a surface susceptibility of the form

$$\bar{\bar{\chi}}^{\mathrm{mm}} = 2\frac{\bar{\bar{\alpha}}^{\mathrm{mm}}}{p^2}, \quad (6)$$

where p is the period of the lattice and where $\bar{\bar{\alpha}}^{\mathrm{mm}}$, given in [8], also includes the effect of rotating electric quadrupoles in addition to that of rotating magnetic dipoles.

Figure 5 plots the normalized admittances for the parameters indicated in the caption. Although this design has not been subjected to optimization, a quasi-perfect free-space PEMC is achieved at 6.11 GHz. Several alternatives to the MNM shown in Fig. 4 could be used for this application, including multilayer MNMs and slot-ring MNMs exhibiting electric (as opposed to magnetic) gyrotropy.

V. GRAPHENE PEMC

Recently, it was discovered that graphene supports giant Faraday rotation, i.e. may, under biasing by a magnetic static field, impart tens of degrees of polarization rotation to a wave propagating across it despite the mono-atomic thickness [10], [11]. This effect is particularly strong at microwave frequencies [10], [12], while novel magnetoplasmons were found to be supported at terahertz frequencie [13].

Figure 6 shows the graphene PEMC structure, which consists of a graphene sheet transferred onto a conductor backed dielectric substrate. As in the ferrite PEMC, the structure is biased by a magnetic static field directed perpendicular to the substrate. Note that the graphene PEMC can be tuned by a gate voltage.
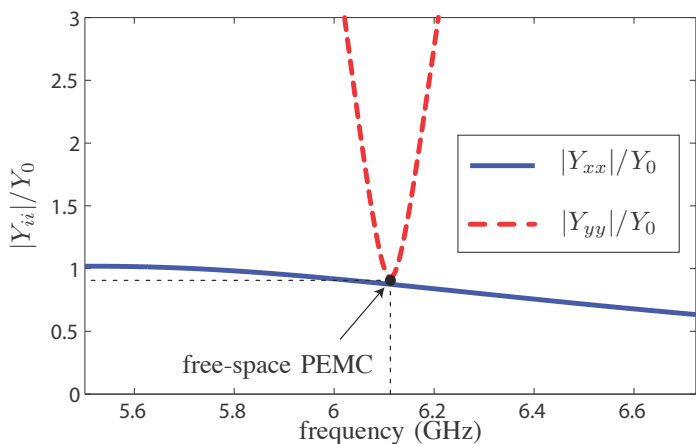
Fig. 5. MNM PEMC admittances versus frequency (exact electromagnetic result) for the following parameters: $\epsilon_r = 2.6$, $h = 0.8$ mm, $R = 5.75$ mm, $w = 2$ mm, ring gap $= 2.5$ mm and $p = 3R$.

Fig. 7. Graphene PEMC admittances versus frequency (exact electromagnetic result) for the following parameters: $\epsilon_r = 3.8$, $h = 500$ μm, $n_s = 1.77 \times 10^{12}$ 1/cm^2 with $\mu = 25{,}000$ cm^2/Vs (a) and $n_s = 1.65 \times 10^{12}$ 1/cm^2 with $\mu = 100{,}000$ cm^2/Vs (b).
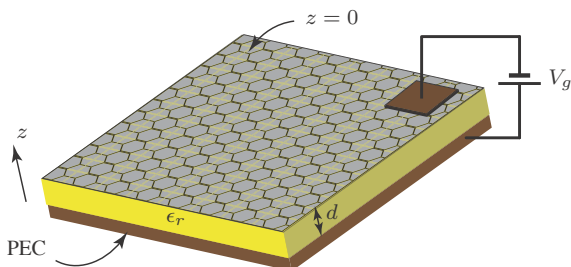

Fig. 6. Graphene PEMC.

Figure 7 plots the normalized admittances for the parameters indicated in the caption. The results are shown for the case of the highest-mobility reported grown graphene ($\mu = 25{,}000$ cm^2/Vs) and for exfoliated graphene ($\mu = 100{,}000$ cm^2/Vs). In the former case, the loss is too high to achieve a PEMC, but the result is not very far from an acceptable free-space PEMC in the latter case. Multilayer graphene-sheet arrangements could yield superior PEMC responses.

VI. CONCLUDING REMARKS

Three Faraday rotation based implementations of PEMC boundaries have been presented: a ferrite PEMC, an MNM PEMC and a graphene PEMC. While the ferrite PEMC boundary has been quite extensively investigated, more research efforts are required in the MNM and graphene PEMC boundaries.

REFERENCES

[1] I. V. Lindell and A. H. Sihvola, "Perfect electromagnetic conductor," *J. Electromagn. Waves App.*, vol. 19, no. 7, pp. 861–869, Jan. 2005.

[2] ——, "Realization of the PEMC boundary," *IEEE Trans. Antennas Propagat.*, vol. 53, no. 9, pp. 3012–3018, Sept. 2005.
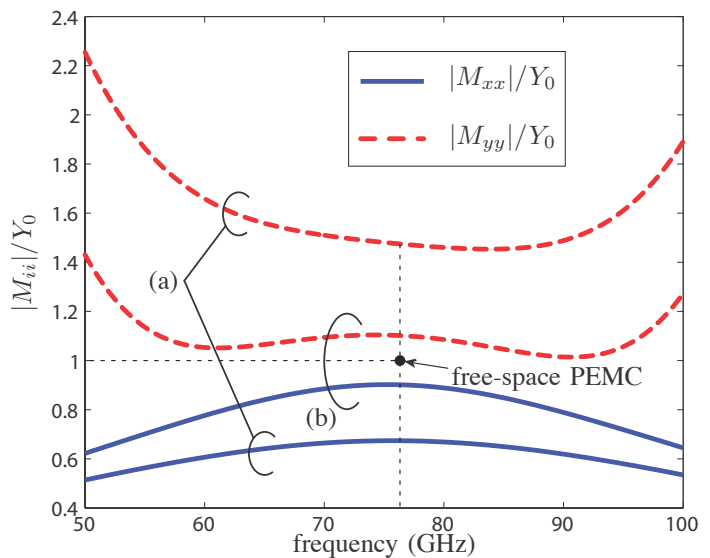
[3] A. Shahvarpour, T. Kodera, A. Parsa, and C. Caloz, "Arbitrary electromagnetic conductor boundaries using faraday rotation in a grounded ferrite slab," *IEEE Trans. Microw. Theory Tech.*, vol. 55, no. 11, pp. 2781–2793, Nov. 2010.

[4] T. Kodera, D. L. Sounas, and C. Caloz, "PEMC metamaterial surface whose gyrotropy is provided by traveling-wave ring resonators," in *IEEE Int. Symp. Antennas Propagat. (ISAP)*, Jeju, South Korea, Oct. 2011.

[5] B. Lax and K. J. Button, *Microwave Ferrites and Ferrimagnetics*. New York, NY: McGraw-Hill, 1962.

[6] L.-P. Carignan, A. Yelon, D. Ménard, and C. Caloz, "Ferromagnetic nanowire metamaterials: theory and applications," *IEEE Trans. Microw. Theory Tech.*, vol. 59, no. 19, pp. 2568–2586, Oct. 2011.

[7] T. Kodera, D. L. Sounas, and C. Caloz, "Artificial Faraday rotation using a ring metamaterial structure without static magnetic field," *Appl. Phys. Lett.*, vol. 99, no. 3, pp. 031 114:1–3, Jul. 2011.

[8] D. L. Sounas, T. Kodera, and C. Caloz, "Electromagnetic modeling of a magnet-less non-reciprocal gyrotropic metasurface," *IEEE Trans. Antennas Propagat.*, in Press.

[9] T. Kodera, D. L. Sounas, and C. Caloz, "Non-reciprocal magnet-less CRLH leaky-wave antenna based on a ring metamaterial structure," *IEEE Antennas Wirel. Propagat. Lett.*, vol. 10, pp. 1551–1554, Jan. 2012.

[10] D. L. Sounas and C. Caloz, "Electromagnetic non-reciprocity and gyrotropy of graphene," *Appl. Phys. Lett.*, vol. 98, no. 2, pp. 021 911:1–3, Jan. 2011.

[11] I. Crassee, J. Levallois, A. L. Walter, M. Ostler, A. Bostwick, E. Rotenberg, T. Seyller, D. van der Marel, and A. B. Kuzmenko, "Giant Faraday rotation in single- and multilayer graphene," *Nature Phys.*, vol. 7, pp. 48–51, 2011.

[12] D. L. Sounas and C. Caloz, "Gyrotropy and non-reciprocity of graphene for microwave applications," *IEEE Trans. Microw. Theory Tech.*, vol. 60, no. 4, pp. 901–914, Apr. 2012.

[13] ——, "Edge surface modes in magnetically biased chemically doped graphene strips," *Appl. Phys. Lett.*, vol. 99, no. 23, p. 231902:13, 2011.